ASTROBIOLOGY
Volume 24, Number 12, 2024

DOI: 10.1089/ast.2024.0096

Simplified Meteorite Parent Body Alteration of Amino Acids by Hydrothermal Processes

Christopher K. Materese,[1] José C. Aponte,[1] Hannah L. McLain,[1–3] Kendra K. Farnsworth,[1,3,4] Patrick D. Tribbett,[1,3,4] Frank T. Ferguson,[1–3] Christine A. Knudson,[1,3,5] Amy C. McAdam,[1] Michael T. Thorpe,[1,3,5] and Jason P. Dworkin[1]

Abstract

Amino acids have been identified in extraterrestrial materials such as meteorites and returned samples from asteroids and comets. Some of these amino acids or their precursors may have formed on icy interstellar dust grains or at a later phase when these grains became incorporated into larger parent bodies. In this work, we simulated parent body aqueous alteration of the residues from irradiated interstellar ice analogs in the presence of relevant minerals (pulverized serpentinite and Allende meteorite). We tracked the change in amino acid abundances as a function of hydrothermal processing time and examined how these differed based on the presence of minerals. We find that the presence of minerals and their mineralogy can have a significant impact on the formation and destruction of amino acids during simulated aqueous alteration experiments. Key Words: Parent body processes—Extraterrestrial amino acids—Aqueous alteration. Astrobiology 24, 1220–1230.

1. Introduction

Chemistry in the molecular cloud that formed our solar system likely played an important role in shaping the primordial inventory of organic compounds (Hagen et al., 1979; Herbst and van Dishoeck, 2009; Öberg, 2016; Materese et al., 2021). In this environment, gases condensed to form icy mantles around sub-micrometer-sized grains while being subjected to ambient radiation. The condensation of molecules onto icy grains in conjunction with the input of energy via radiation facilitated the formation of complex organic molecules that would not have readily formed in the gas phase. Over time, some of these icy grains became sequestered into larger bodies. In these larger bodies, ices and more complex organic radiolysis products may have been subjected to hydrothermal alterations (Kebukawa et al., 2017; Vinogradoff et al., 2020b; Qasim et al., 2023), further altering their composition.

Carbonaceous chondrites provide a window into the chemical inventory of the early solar system, and their contents were likely influenced by a combination of inheritance from the materials from the Solar Nebula, including icy grains and parent body processes such as aqueous alteration. Amino acids are among the myriad of compounds detected in extracts from carbonaceous chondrites (Burton et al., 2012; Cobb and Pudritz, 2014; Elsila et al., 2016; Glavin et al., 2018) and are of particular interest for their astrobiological relevance. Amino acids have also been detected in the room temperature residues of laboratory ice photolysis (Briggs et al., 1992; Bernstein et al., 2002; Muñoz Caro et al., 2002; Nuevo et al., 2007, 2008; de Marcellus et al., 2011) and particle radiation experiments that simulate the chemistry of icy grains (Kasamatsu et al., 1997; Takano et al., 2007; Hudson et al., 2008, 2009).

Notably, the distribution of amino acids and amines in these residues is not consistent with what has been detected in meteorites. It has been hypothesized that the amino acids in meteorites may be produced by a combination of ice radiation chemistry and hydrothermal processes in the parent body (Chang and Bunch 1986; Shock and Schulte 1990;

[1]Solar System Exploration Division, NASA Goddard Space Flight Center, Greenbelt, Maryland, USA.
[2]Department of Chemistry, Catholic University of America, Washington, District of Columbia, USA.
[3]Center for Research and Exploration in Space Science and Technology, NASA GSFC, Greenbelt, Maryland, USA.
[4]Center for Space Science and Technology, University of Maryland Baltimore County, Baltimore, Maryland, USA.
[5]Department of Astronomy, University of Maryland College Park, College Park, Maryland, USA.

Aponte et al., 2017a; Aponte et al., 2017b). Consequently, although some amino acids in meteorites may have been directly inherited from the radiation chemistry on icy grains, hydrothermal alteration of organic material in parent bodies likely played an important role in the distribution of amino acids found in meteorites.

Looking at amino acid synthesis from a "top-down" perspective starting with complex precursors, Vinogradoff et al. (2018), Vinogradoff et al. (2020a), and Vinogradoff et al. (2020b) investigated the hydrolysis of hexamethylenetetramine (HMT) as a potential source for amino acid synthesis in asteroids during aqueous alteration. Notably, HMT and its derivatives are known to be among the most abundant products identified in residues when ices that contain C, H, O, and N are irradiated (Bernstein et al., 1995; Cottin et al., 2001; Muñoz Caro and Schutte, 2003; Oba et al., 2017; Materese et al., 2020) and could be considered a simplified analog of these residues. Vinogradoff et al. (2020a) and Vinogradoff et al. (2020b) analyzed the hydrolysis of HMT under conditions designed to simulate asteroidal aqueous alteration. Specifically, HMT was hydrolyzed in water at 150°C alone and in water mixed with phyllosilicate minerals (Al- or Fe-rich smectites) for up to 31 days. Their results demonstrated that hydrolysis of HMT in the presence of Al-rich smectites appeared to promote the formation of amino acids, while similar hydrolysis in the presence of Fe-rich smectites suppressed their formation. Overall, these findings suggest that the presence of minerals could play a key role in the synthesis of organic compounds in asteroids.

In contrast, Kebukawa et al. (2017) and Elmasry et al. (2021) simulated amino acid formation from a "bottom-up" framework operating through base-catalyzed formose reactions, starting with a solution of simple precursor molecules (H_2CO, NH_3, H_2O and glycolaldehyde in the former experiments only). In Elmsry et al. (2021), amino acids were also synthesized from their precursor mixture alone and in the presence of minerals, namely olivine, Na-montmorillonite, or serpentine, at 150°C for up to 7 days. Their findings suggest that the presence of minerals provided a short-term boost (up to 3 days depending on the mineral) to the formation of amino acids from simple precursors relative to those formed in their absence, but later enhanced amino acid decomposition by the end of their experiments on day 7.

In our previous work, we performed simplified experiments to examine hydrothermal alterations of complex organic residues generated from ice radiolysis experiments (Qasim et al., 2023). In these experiments, we irradiated commonly observed interstellar gas mixtures, and their residues were recovered, dissolved in water, divided, subjected to processing at varying temperatures and times, and sampled at several intervals up to 30 days to monitor changes in their amino acid and amine contents. The results of these experiments suggest that, although inheritance of amino acids and amines from the residues was still an important factor after 30 days, hydrothermal processing had a measurable influence on their abundances (Qasim et al., 2023).

The work presented here expands on our prior experiments by including minerals relevant to carbonaceous chondrites during the hydrothermal processing to test whether their presence has an impact on the production or destruction of amino acids. Specifically, our samples included pulverized samples of the Allende meteorite (a CV3 chondrite that consists mostly of olivine) and serpentinite (a metamorphic rock dominantly composed of serpentine minerals). The hydrothermal processing of our samples was conducted with and without the presence of these minerals to evaluate their impact on the abundance of amino acids over time.

2. Experimental Methods

All glasswares discussed throughout this methods section were first cleaned by rinsing with Milli-Q ultrapure water (hereafter "water"; 18.2 MΩ, <3 ppb of total organic carbon) and then baked in a furnace at 500°C in air overnight.

2.1. Allende and serpentinite removal of organics

Samples of the Allende meteorite (Smithsonian Institution) and serpentinite (Lancaster County, PA, USA) were first crushed and then cleaned by placing roughly 1 g of each material in short pipettes tampered with quartz wool. The mineral samples were rinsed in sequence by using three pipette volumes of HPLC-grade methanol and water. The methanol–water rinses were dried and heated at 500°C for 16 h to remove organic matter. Then, the pyrolyzed residue (composed of mostly water-soluble salts) was redissolved in water. These organic-free solutions were added back to the mineral samples and were then dried using centrifugal rotation at reduced pressures (Labconco CentriVap) and room temperature for 72 h. The mineral powders were tested for their organic content by using pyrolysis gas chromatography coupled with mass spectrometry, which showed the absence of soluble organics and organic macromolecules.

2.2. Allende and serpentinite surface area measurements

Specific surface area measurements were made on the pulverized Allende and serpentinite samples by using a Quantachrome Nova 2200e surface area and pore size analyzer.

Approximately 1 g of each sample was used during the test, and each sample was degassed under vacuum prior to the surface area measurements. To avoid thermal alteration of the samples, they were held at room temperature, under vacuum, for 18 h during degassing. Allende and serpentinite samples were held at liquid nitrogen temperatures and exposed to nitrogen gas at different ratios of the nitrogen saturation pressure, and the specific surface area was determined by performing a Brunauer–Emmett–Teller (BET) isotherm analysis (Brunauer et al., 1938; Sing, 1998) of the adsorption data. In this analysis, five adsorption points within the so-called "linear region" were measured where the ratio of the equilibrium pressure to the saturation pressure (p/p_0) ranges from 0.05 to 0.3. The adsorption measurements for both samples provided good fits to these BET plots, and the specific surface area of the Allende sample was measured at 1.65 m^2/g, while the serpentinite sample was 1.41 m^2/g. These results suggest that the overall surface areas of the Allende and serpentinite powders in our samples were very similar.

2.3. X-ray diffraction analyses of Allende and serpentinite

The compositions of the mineral samples were determined by X-ray diffraction analyses on a Bruker D8 Discover X-

ray diffractometer. The patterns were acquired on the fine powders from 2 to 70°2θ (Cu Kα radiation, λ = 1.54059 Å), and quantitative mineralogy was obtained by Rietveld refinement methods using the MDI (Materials Data Incorporated) Jade analysis software. The Allende meteorite sample was composed of 72 wt. % olivine and 28 wt. % clinopyroxene (Fig. 1). The serpentinite was dominantly serpentine minerals of about 87 wt. % (lizardite/antigorite), 7.5 wt. % olivine, 1.5 wt. % magnetite, 1 wt. % hydrotalcite, and 3 wt. % brucite (Fig. 1).

2.4. Radiolysis experiments

All ice radiolysis steps were conducted in a high-vacuum chamber ($\sim 2 \times 10^{-7}$ torr at room temperature, $\sim 6 \times 10^{-8}$ torr at 25K). The vacuum chamber is attached to a gas manifold with multiple inlet ports, which allows each compound in the ice mixture to remain isolated until it is condensed onto the substrate. The vacuum chamber is coupled to a Van de Graaff accelerator, which is capable of irradiating samples with 0.9 MeV p^+.

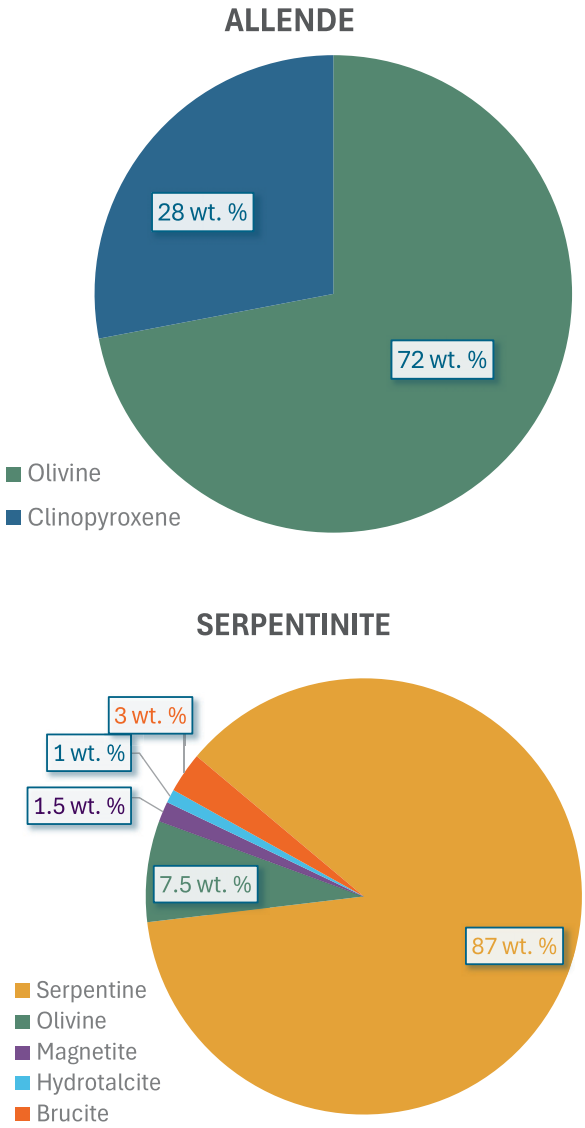

FIG. 1. The compositions of the rocks used for simulated hydrothermal processing as determined by X-ray diffraction analysis.

Ice films were generated through vapor deposition of gases onto a clean aluminum foil substrate (heated in air to 500°C for 24 h prior to use) that was attached to a closed-cycle helium cryocooler with a copper gasket and cooled to 20K. All sample ices, H_2O:CO_2:CH_3OH:$HC^{15}N$ (20:4:2:1), were grown for $\sim$3 h to a thickness of 15 μm using methods described by Qasim et al. (2023). Nitrogen-15 labeling of the HCN was used to ensure that any amino acids produced during radiolysis or during later hydrothermal processing could be differentiated from possible sources of contamination. All reactants except for $HC^{15}N$ were obtained commercially: H_2O (Fisher Chemical, HPLC grade), CO_2 (Matheson, 99.8%), and CH_3OH (Sigma-Aldrich, HPLC grade). To obtain $HC^{15}N$, we used the method described by Gerakines et al. (2004). Briefly, $HC^{15}N$ gas was synthesized by the reaction of a mixture of $KC^{15}N$ (Sigma-Aldrich, 98% 15N) and stearic acid [$CH_3(CH_2)_{16}COOH$, Sigma-Aldrich, reagent grade] powders in roughly equal molar ratio. The mixture was heated to 350 K under vacuum and held at that temperature until the reaction was complete. The reaction yielded $HC^{15}N$ and CO_2 gases, which were collected in a bulb. The bulb was then cooled to 77 K by liquid N_2 and then warmed to 178 K in an acetone slush bath and the CO_2 was pumped away.

After deposition, the samples were irradiated with 0.9 MeV p^+ to a dose of $\sim$10 eV/molecule. The radiation received by our samples simulates a radiation dose that ice grains would experience prior to sequestration into a larger planetary body (10^7 years; average lifespan of a dense molecular cloud; Moore et al., 2001; Blitz and Shu, 1980; Behr et al., 2020) prior to sequestration into a larger planetary body. An equivalent dose was used in our previous work (Qasim et al., 2023). After irradiation, the samples were gradually warmed to 300 K at a rate of 1.5 K/min to slowly release volatiles, which left behind refractory organic residues. The foils containing these residues were quickly recovered, transferred to prebaked glass vials, and immediately stored in a −80°C freezer prior to use in the simulated hydrothermal processing experiments. In total, six residues were generated using the same conditions. These six residues allowed subsequent hydrothermal processing experiments to be performed in duplicate.

Two control samples were created: (1) ice without radiation and (2) radiation without ice. These controls were used to mitigate potential contamination in the radiation and ice formation steps.

We note that HCN was chosen as our nitrogen source in our initial ices unlike the NH_3 used in our previous experiments. This choice was made in the hopes of generating some larger amino acids that could be identified and quantified in our initial unprocessed samples and to discern whether there was any change in the relative initial abundances of α- versus β-amino acids. Ultimately, the substitution of HCN for NH_3 did not yield anything of note.

2.5. Hydrothermal processing experiments

The vials that contained residues from the radiolysis experiments were extracted from the −80°C freezer and warmed to room temperature. To each vial, 1 mL of methanol

(Fisher Chemical, HPLC grade) was added, and the samples were sonicated for 10 min. The liquid contents of each vial were transferred to prebaked 10 × 32 mm vials (Supelco) that contained 10 μL of 6M HCl (Tama Chemicals Co., Ltd., ultrapure) to preserve volatile amines that could potentially form amino acids in the subsequent hydrothermal processing steps. Four 200 μL aliquots of each sample were transferred to prebaked 13 × 100 mm borosilicate tubes (Kimble). After all samples were divided and transferred to the borosilicate tubes, they were dried at reduced pressures for 24 h to remove methanol. Depending on the sample type, water and Allende, water and serpentinite, or water alone were added to the sample tubes. Sample tubes were attached to a vacuum manifold, and the samples were frozen in liquid nitrogen and degassed three times by using a freeze–pump–thaw cycle. Finally, samples were flame-sealed under vacuum as described in the work of Pavlov et al (2022) and returned to the −80°C freezer until needed. The first of these four tubes was designated to receive no hydrothermal processing beyond being dissolved in water at room temperature and then immediately refrozen at −80°C until analysis. The remaining three tubes were used for hydrothermal processing at 125°C for 2, 7, and 30 days, respectively. All four tubes corresponding to a particular residue's sample (*i.e.*, 0, 2, 7, and 30 days) were then designated for one of three possible hydrothermal processing conditions: (1) in 200 μL of water only, (2) in 200 μL of water with 50 mg pulverized Allende powder, and (3) in 200 μL of water with 50 mg pulverized serpentinite. The temperature and duration of the experiments were chosen to match our previous experiments in Qasim et al. (2023).

An additional three sets of blank experiments (four samples each, for 0 days, 2 days, 7 days, and 30 days) were created where 200 μL of ultrapure water was pipetted into a sample tube with no additional minerals, with 50 mg of pulverized Allende, or 50 mg of pulverized serpentinite. These procedural blanks were designed to test for amino acid contamination, especially any contamination that could have come during residue transport, drying, and setup, or from sample separation (tube breaking) before analyses.

The pH of the samples was controlled primarily by the added minerals and was measured prior to the addition of the residues using pH paper. The starting pH of water alone was 7.0, mixtures of water with pulverize Allende was 7.9, and water with pulverized serpentinite was 9.0. No buffers were added to artificially control the pH so that the analysis could focus directly on the influence of the minerals surfaces and ions they released into the solution.

Samples were heated in a laboratory oven at 125°C for 2, 7, or 30 days without interruption. After heating, samples were immediately returned to the −80°C freezer until analysis. The samples referred to as "0 days" remained in the freezer undisturbed until analysis. After all hydrothermal processing experiments were complete, all sample tubes were carefully broken open, liquids were pipetted out, and transferred to baked 12 × 32 mm recovery tubes. An additional 0.5 mL of water was pipetted into the sample tube and transferred to the recovery tubes twice to recover as much residual material as possible. No acid hydrolysis was performed on the samples after simulated aqueous alteration.

2.6. Liquid chromatography–mass spectrometry analysis after hydrothermal processing

All commercially purchased reagents used were acquired from Sigma-Aldrich, Fisher Scientific, Acros Organics, Combi-Blocks, Bachem, Tokyo Chemical Industry, and Waters Corporation. Amino Acid Hydrolysate H from Waters was utilized along with stock amino acids prepared by dissolving individual analyte crystals (purities ranged from 96% to 100%) in ultrapure water. Stock amino acid standard solutions were made with concentrations ranging from 0.01 to 1M. This standard set included the 20 protein amino acids, plus the nonprotein amino acids, β-Alanine γ-ABA, β-ABA, β-AIB, α-AIB, and α-ABA (Supplementary Fig. S1; Supplementary Table S1).

The portions of the water extract allocated for amino acid analyses were dried under vacuum and then derivatized with AccQ·Tag using previously described methods (*e.g.*, Vinogradoff et al., 2020b). Each sample was resuspended in ultrapure water, and 10 μL was used for AccQ·Tag derivatization, which was performed as follows: (1) adding 70 μL sodium borate buffer, 10 μL sample, and 20 μL AccQ·Tag derivatization agent to a total recovery vial, (2) heating at 55°C for 10 min, and (3) injecting 1 μL into the liquid chromatography–mass spectrometry. Standards that consisted of a set of eight calibrators of amino acids were prepared in water and processed identically to the samples.

The derivatized amino acid extracts were analyzed via the commercial Waters AccQ·Tag protocol on a Xevo TQS-Micro triple quadrupole mass spectrometer equipped with an electrospray ionization source (positive ion mode) using multiple reaction monitoring (MRM) mode. The Xevo TQ-S Micro capillary voltage was set to 1.0 keV, the sampling cone was set to 40°C, the source temperature was set to 150°C, the cone gas flow was set to 50 L/h, the desolvation temperature was set to 500°C, and the desolvation gas flow was set to 1000 L/h. Samples were introduced via a Waters Acquity H-Class plus Ultra High Precision Liquid Chromatography (UHPLC) with a fluorescence detector.

UHPLC separations were performed by using an AccQ·Tag Ultra C18, 1.7 μm. 2.1 × 150 mm column. Amino acid target analytes were eluted by using the following gradient: 0–2.49 min: 0–10% eluent B, 2.49–7 min: 10–20% eluent B, 7–7.99 min: 20–50% eluent B, 8–8.99 min: 100% eluent B, 8.99–9 min: 100–0% eluent B, 9–10 min: 0% eluent B. The autosampler temperature was maintained at 25°C, the injection volume was 1 μL, the eluent flow rate was held at a constant 0.7 mL min^{-1}, and the column was maintained at 55°C. The fluorescence detector was operated with an excitation wavelength of 266 nm and an emission wavelength of 473 nm.

Selected MRM transitions were used for amino acid quantifications (Supplementary Table S1). A linear least-square model was fitted to each amino acid in the standard calibration set, and these calibration curves were used to quantify the analytes in the samples. A sample of pure water that was carried through the same preparation and analytical procedures as the samples was used as a blank to determine the procedural and laboratory backgrounds. All derivatized extracts were analyzed in triplicate, and the average blank-corrected amino acid concentrations of the

samples were determined from the standard calibration set and the extracted sample mass.

Sarcosine was not included in the original standard set, but its analysis was included *post hoc*. For sarcosine identification, we spiked the 1364 Allende 30-day sample with a sarcosine standard to verify an identical retention time of the standard to the suspected sarcosine peak observed in the sample (Supplementary Fig. S2). For sarcosine quantification, we used a calculated coefficient to normalize the sarcosine standard peak area to the β-alanine peak area at a concentration of 25 μM. We then used the normalized standard peak areas to structure a sarcosine calibration curve and calculate the associated concentrations.

3. Results

Five amino acids, glycine, serine, α-alanine, β-alanine, and sarcosine were detected in our samples, and the concentrations are reported in Table 1. The first four amino acids were the most abundant amino acids detected in our previous work (Qasim et al. 2023), but no attempt was made to detect or quantify sarcosine in the previous study. The only source of nitrogen in our original ices was ^{15}N-labeled HCN so the m/z peak associated with the ^{15}N-isotopologue of each amino acid was used for identification and quantification. As an additional check, the m/z peaks associated with the ^{14}N-amino acid isotopologue were also measured (Supplementary Fig. S3), and in all cases, the [^{15}N] was at least twice the [^{14}N]. This result eliminates the possibility that a significant portion of the m/z associated with ^{15}N-amino acids could have been natural levels of ^{13}C from unintentional amino acid contamination.

^{15}N-amino acids were not detected in either of the procedural blanks—nonirritated ices and the irradiated "no ice" controls. Glycine, serine, β-alanine, and sarcosine were not detected in any of the samples from our blank experiments. Although ^{15}N-α-alanine was not detected in any of the 0-day samples, it was detected in the 2-, 7-, and 30-day blank samples at concentrations roughly an order of magnitude lower than what was detected in the nonblank samples. Notably, the concentrations of ^{15}N-α-alanine in the blank samples are nearly identical regardless of the presence of minerals, which suggests that the minerals are not the source of this contamination.

It is normal for some variation to occur between samples despite the significant efforts taken to ensure that experimental conditions were identical for ice deposition, radiolysis, and residue recovery. Sample recovery is far easier and more efficient from the sample vials that contain only water relative to those that contain water and minerals. This effect is demonstrated by the fact that, for each amino acid, the 0-day concentrations observed in the water-only samples are all larger than those observed for the samples containing minerals. The 0-day concentrations of amino acids recovered from the samples containing Allende are slightly lower, but mostly within the margin of error (for all but sarcosine) when compared to the concentration of those recovered from samples containing serpentinite. This is consistent with the Allende powder's marginally larger 1.65 m^2/g surface area compared with serpentinite's 1.41 m^2/g. Because of these natural variations and differences in sample recovery, we examined the percent change (Δ%) relative to their 0-day values (Fig. 2) to best understand how the amino acid concentrations evolve during hydrothermal alteration. Overall, hydrothermal processing had a significant impact on the abundance of amino acids in our samples, but the effects varied significantly based on the specific amino acids in question and on the presence of minerals. The abundance of each amino acid studied regardless of the presence of minerals (with the possible exception of serine in water alone) increased significantly between the unprocessed (0 days) and those exposed to 2 days of hydrothermal processing. This was likely mostly driven by the hydrolysis of amino acid precursors present in the residue. After two days, the change in the abundances of the amino acids varied much more significantly based on amino acid type and the presence of minerals.

3.1. Glycine

The Δ% [(2 days, 7 days, or 30 days)/(0 days)] of glycine appears to significantly increase after 2 days of hydrothermal processing (Fig. 2A). The Δ% of glycine appears to increase somewhat more in samples containing pulverized Allende or serpentinite than it does in water alone for 2 days, but large error bars for water and serpentinite make this difficult to confirm. After 7 days, the abundance of glycine remained unchanged, within the margin of error, up to the end of the experiment at 30 days. Overall, the abundance of glycine is relatively stable throughout the experimental time frame. By the end of the 30-day experiments, the abundance of glycine appears largely unaffected by the presence or absence of minerals in the sample tube.

3.2. Serine

Unlike glycine, the Δ% of serine varies significantly as a function of both hydrothermal processing time and the presence and identity of minerals in the sample tube (Fig. 2B). For samples containing only water, the abundance of serine remains largely unchanged from its initial level within the margin of error throughout the experiment. In contrast, when the sample contained pulverized Allende powder, the abundance of serine at 2 days increased nearly threefold. After that, it remained near the 2-day abundance at day 7 before declining to about 150% of its initial value at 30 days. When samples contained serpentinite, the abundance stayed the same, or increased slightly after 2 days of hydrothermal processing; however, it then consistently declined to only a small fraction of its initial abundance by the end of the experiment.

3.3. α-Alanine

For all samples, at the end of 2 days regardless of the presence of minerals, the Δ% of α-alanine initially increases in a similar fashion by two-fold or more from its initial abundance. After this initial increase (Fig. 2C), the abundance of α-alanine continues to rise indistinguishably within the margin of error for the remainder of the experiment for samples containing only water and samples containing pulverized Allende. In contrast, after 2 days the abundance of α-alanine in samples containing serpentinite steadily declined throughout the rest of the experiment back to its initial abundance by day 30.

Table 1. Amino Acid Concentration Overview

Sample	0 days			2 days			7 days			30 days		
	Concentration (μM)	*Average concentration (μM)*	*Standard deviation (μM)*	*Concentration (μM)*	*Average concentration (μM)*	*Standard deviation (μM)*	*Concentration (μM)*	*Average concentration (μM)*	*Standard deviation (μM)*	*Concentration (μM)*	*Average concentration (μM)*	*Standard deviation (μM)*
Glycine												
Water 1	87.5	107	27.6	140	137	4.58	150	154	5.59	158	163	7.25
Water 2	127			133			158			168		
Allende 1	50.0	62.0	16.9	101	119	26.5	107	116	12.6	82.1	100	25.9
Allende 2	73.9			138			125			119		
Serpentinite 1	59.0	67.6	12.2	149	144	7.28	105	126	29.7	105	118	18.0
Serpentinite 2	76.3			139			147			130		
Blank (w)	n.d.	—	—	n.d.	—	—	n.d.	—	—	n.d.	—	—
Blank (A)	n.d.	—	—	n.d.	—	—	n.d.	—	—	n.d.	—	—
Blank (S)	n.d.	—	—	n.d.	—	—	n.d.	—	—	n.d.	—	—
Serine												
Water 1	13.3	14.1	1.06	18.1	17.4	0.980	16.8	17.8	1.39	12.1	13.7	2.22
Water 2	14.8			16.7			18.8			15.2		
Allende 1	4.10	4.95	1.20	11.7	14.4	3.82	11.6	12.9	1.94	6.40	8.06	2.34
Allende 2	5.80			17.1			14.3			9.72		
Serpentinite 1	4.40	6.05	2.33	8.60	8.65	0.0712	2.27	3.94	2.36	0.804	0.897	0.131
Serpentinite 2	7.70			8.70			5.61			0.989		
Blank (w)	n.d.	—	—	n.d.	—	—	n.d.	—	—	n.d.	—	—
Blank (A)	n.d.	—	—	n.d.	—	—	n.d.	—	—	n.d.	—	—
Blank (s)	n.d.	—	—	n.d.	—	—	n.d.	—	—	n.d.	—	—
α-alanine												
Water 1	2.28	2.46	0.256	5.85	5.16	0.977	7.65	7.69	0.057	9.69	9.77	0.113
Water 2	2.64			4.47			7.73			9.85		
Allende 1	1.04	1.28	0.339	2.86	3.61	1.07	3.54	3.94	0.560	3.80	4.59	1.11
Allende 2	1.52			4.37			4.33			5.38		
Serpentinite 1	1.74	1.75	0.019	4.37	4.15	0.314	2.80	3.08	0.407	2.02	1.97	0.0699
Serpentinite 2	1.76			3.92			3.37			1.93		
Blank (w)	n.d.	—	—	0.4	—	—	0.4	—	—	0.4	—	—
Blank (A)	n.d.	—	—	0.4	—	—	0.4	—	—	0.5	—	—
Blank (s)	n.d.	—	—	0.4	—	—	0.4	—	—	0.4	—	—
β-alanine												
Water 1	1.66	2.00	0.484	2.96	2.85	0.154	2.37	2.44	0.099	0.378	0.469	0.128
Water 2	2.34			2.74			2.51			0.559		
Allende 1	0.530	0.817	0.405	1.44	2.09	0.923	0.965	1.26	0.421	n.d.	—	—
Allende 2	1.10			2.74			1.56			n.d.		
Serpentinite 1	1.29	1.28	0.0211	2.85	2.89	0.0542	1.19	1.39	0.293	n.d.	—	—
Serpentinite 2	1.26			2.93			1.60			0.521		
Blank (w)	n.d.	—	—	n.d.	—	—	n.d.	—	—	n.d.	—	—
Blank (A)	n.d.	—	—	n.d.	—	—	n.d.	—	—	n.d.	—	—
Blank (s)	n.d.	—	—	n.d.	—	—	n.d.	—	—	n.d.	—	—
Sarcosine												
Water 1	92.1	93	1.3	169.4	152	24.44	188.3	177	15.35	211.1	198	18.41
Water 2	94.0			134.8			166.5			185.1		
Allende 1	37.7	45.4	10.9	106.6	135	39.5	112.3	124	16.1	85.5	106	29.0
Allende 2	53.1			162.4			135.2			126.6		
Serpentinite 1	83.0	81.5	2.2	194.5	182	18.02	138.6	158	27.6	144.9	154	12.4
Serpentinite 2	79.9			169.0			177.5			162.5		
Blank (w)	n.d.	—	—	n.d.	—	—	n.d.	—	—	n.d.	—	—
Blank (A)	n.d.	—	—	n.d.	—	—	n.d.	—	—	n.d.	—	—
Blank (S)	n.d.	—	—	n.d.	—	—	n.d.	—	—	n.d.	—	—

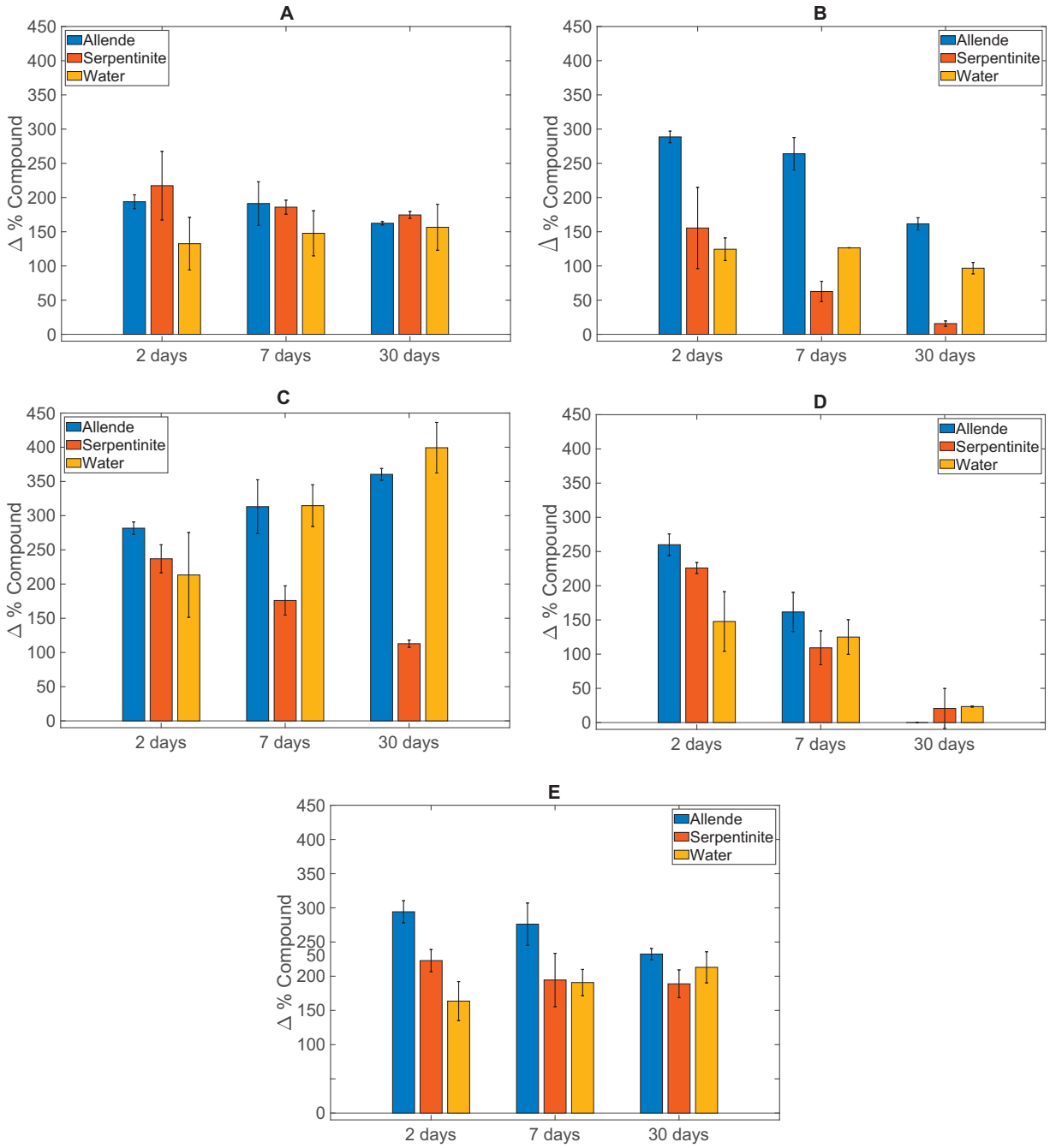

FIG. 2. Change in product abundances after aqueous alteration of the residues for **(A)** glycine, **(B)** serine, **(C)** α-alanine, **(D)** β-alanine, and **(E)** sarcosine. All values are normalized to their initial (0 days) values (see the "Methods" Section).

3.4. β-Alanine

At the end of 2 days, the Δ% of β-alanine initially increases by over 200% for samples containing pulverized Allende and serpentinite powders and increases by approximately 150% with a relatively large margin of error for samples containing only water. After 2 days, the abundance of β-alanine steadily decreases for the remainder of the experiment for all samples at a similar rate within the margin of error (Table 1, Fig. 2D). The lower β-alanine abundances with increasing aqueous processing were also observed from our previous work (Qasim et al., 2023) and was explained at least in part by the lack of α-β-nitriles in the residue synthesis.

3.5. Sarcosine

The Δ% of sarcosine appears to significantly increase after 2 days of hydrothermal processing (Fig. 2E) and then does not appear to experience significant changes with additional processing. The notably Δ% of sarcosine does appear to increase somewhat after 2 days, for samples containing pulverized Allende than for samples containing serpentinite or water alone, but all converge on the same concentration at the end of the 30 days. Notably, sarcosine is one of the most abundant amino acids detected in our samples, sometimes exceeding the abundance of glycine.

4. Discussion

In almost all cases with the possible exceptions of glycine and serine in water alone, the abundance of each amino acid increases significantly from its initial 0-day value to the 2-day samples. These data suggest that, initially, the synthesis of amino acids is strongly favored. The relative abundances of amino acids changed over time for samples that contained water alone, which shares some similarities to the results of Qasim et al. (2023), but there are some differences in the amino acid abundances. Although we observed the same general trend of glycine $\gg$ serine > α-alanine > β-alanine, there are differences in how their abundances evolved over time. In the work of Qasim et al. (2023), at the end of 2 days at 125°C, the Δ% of glycine was somewhat unchanged but grew significantly by day 7, followed by a subsequent decline. In contrast, in the current experiments, the Δ% for glycine in all samples grew modestly by 2 days and remained mostly unchanged for the duration of the 30-day experiment. Another difference is that the Δ% of β-alanine declines significantly at the end of 30 days in the current experiment, while in the previous study, it had returned to roughly its initial value after an initial increase after the same duration. The observed variation in the abundances of some amino acids in this, and our previous work, may be caused by a difference in the initial ice compositions between experiments. Specifically, in the current experiments, HCN replaced NH_3 from the prior experiments as the sole source of nitrogen. Note that the abundance of sarcosine was not quantified in our previous work and, therefore, no direct comparison can be made.

One possible source of amino acid synthesis is the hydrolysis of complex molecules such as HMT and its derivatives, which as previously mentioned are often among the most abundant products of the irradiation or photolysis of interstellar ice analogs. Indeed, Hulett (1971) demonstrated that glycine, α-alanine, and serine respectively were the three most abundant amino acids produced by the hydrolysis of HMT under acidic conditions. However, synthesis from HMT is likely only part of the explanation for the changes in amino acids observed in our experiments. In the work of Vinogradoff et al. (2018), HMT abundance was tracked throughout their 150°C hydrolysis experiments and was no longer detected between their 7- and 20-day samples. This suggests that, if HMT plays a role in amino acid synthesis in our samples, its influence may no longer be significant sometime after 7 days. As previously stated, Vinogradoff et al. (2020a) and Vinogradoff et al. (2020b) examined the formation of amino acids from HMT with and without the addition of Al- and Fe-rich smectites (phyllosilicates), and significant differences in amino acids abundances were observed between this study and Vinogradoff et al. (2020a) and Vinogradoff et al. (2020b). First, serine was not detected in their samples at above blank levels, while it was the second most abundant amino acid in ours. Although a trend of glycine $\gg$ α-alanine > β-alanine was observed in their experiments, their abundances all gradually increased for the entire 31-day duration of their experiments (with and without the presence of smectites) while, in contrast, we generally observed the largest increases in abundance after just 2 days followed by minimal-to-modest increases or even declines. Interestingly, although Vinogradoff et al. (2020b) observed that Al-rich smectites appeared to promote amino acid formation and Fe-rich smectites appeared to suppress amino acid formation, a decline in the abundance of amino acids with increased hydrothermal processing time was not observed in any of their experiments. This stands in contrast with our results (Fig. 2), where after 2 days the presence of the serpentinite appears to promote the destruction of serine and α-alanine.

Although the starting materials of our samples are dissimilar from the simple precursor studied by Elmasry et al. (2021), there are some notable similarities between our results. First, the presence of olivine or serpentine in their samples appears to promote the formation of glycine, serine, and α-alanine after up to day 3 of their experiments. Our 2-day samples (Fig. 2) are consistent with this trend, though it is important to be mindful of the margin of error. Interestingly, by 7 days the presence of either olivine or serpentine in samples discussed in Elmasry et al. had a minimal impact on glycine abundance relative to their 3-day values, a finding similar to our results. Notably, there are also significant differences in our results as well, namely the presence of serpentinite appears to have a negative impact on the abundance of serine, a result that was not observed by Elmasry et al. (2021). Another significant difference with regard to Elmasry et al. (2021) is the continual decline in the abundance of β-alanine regardless of the presence of minerals in our samples.

The abundances of serine, α-alanine, and possibly β-alanine are enhanced in Allende powder relative to serpentinite, at least for the first 7 days (Fig. 2). These observations may be related to two independent, though not mutually exclusive factors: (1) the polarity and/or water solubility of the amino acids and (2) the charge of the mineral surfaces in the Allende and serpentinite powders during aqueous processing, that is, the release of ions to solution due to mineral dissolution, the formation/destruction of reaction sites on the mineral.

Mineral dissolution affects the pH of the sample and surface charge which can impact the organic chemistry that occurs in solution. The presence of serpentinite in water created alkaline initial conditions (pH = 9.0), and the serpentine fraction was likely negatively charged during the experiment, as Mg^{2+} was released to the solution (Li et al., 2023). The presence of pulverized Allende created slightly alkaline conditions (pH = 7.9), and the surfaces of the olivine and pyroxene were likely slightly negatively charged, as they also would have released metal cations such as Mg^{2+} to solution, as well as Si in the form of as SiO_2(aq) (Hänchen et al., 2006; Wogelius and Walther, 1991).

The higher charge surfaces of the serpentine in the serpentinite sample may have preferentially adsorbed polar organic compounds such as amino acids as compared to the surfaces of the olivine and pyroxene in Allende. This effect may also partially explain the trends in the amino acid abundances over time in the serpentinite experiments. For example, the solution concentrations of the less polar (and relatively more water soluble) glycine show a less pronounced decline over time than the more polar (but relatively less water soluble) serine, which may be more effectively adsorbed to the charged mineral surface. Adsorption of amino acids or other organic compounds in solution to mineral surfaces could

catalyze chemistry through hydrolytic breakdown from reactions with surface OH (Kleber et al., 2021). Additionally, amino acid adsorption could hinder their recovery and extraction for analysis, which in turn could alter their apparent abundances. This effect, however, cannot explain the decline in abundance of α-alanine in samples containing serpentinite relative to those containing pulverized Allende or water alone. It is also possible that the cations released to solution due to partial dissolution of the mineral samples may have affected the abundances of amino acids detected. Cations such as magnesium can form chelates or other compounds with amino acids, which could impact their detection. However, it is challenging to invoke a chelating mechanism that would be specific to α-alanine and none of the other amino acids studied here. Mineral-driven differences in pH between the samples likely also played a role in the efficiency of amino acids synthesis or destruction.

Amino acid synthesis from nitriles likely plays an important role in our samples, especially with HCN as part of the reactant ices. Strecker synthesis, Michael addition, Maillard reaction, and HCN polymerization are all potentially important mechanisms for this synthesis. Like the findings of our previous work, the greater abundance of α-alanine versus β-alanine suggests that the Strecker synthesis may play a more significant role than Michael addition.

In current experiments, we observed a decrease in β-alanine concentration with increasing hydrothermal processing time. Unlike our previous work (Qasim et al. 2023), we used $HC^{15}N$ in the present study as one of the starting materials for the synthesis of the irradiated residue, thus, we expected that amino acids, especially β-alanine, would form from the Michael addition to α-β-unsaturated nitriles. Our results suggest that α-β-unsaturated nitriles may be present during ice irradiation and the first days of hydrothermal processing; however, the rapid decrease of β-alanine with aqueous alteration is challenging to explain. This is of particular interest because of the larger β-alanine contents observed in meteorites with increasing aqueous alteration (Glavin et al., 2011, 2020). Thus, it could be argued that the concentration of β-alanine in meteorites may not be fully affected by aqueous processing but by the availability of starting materials such as α-β-unsaturated nitriles during the accretion of the parent body.

5. Conclusion

Our results suggest that the presence of minerals during aqueous alteration could have a significant impact on the abundances of amino acids inherited from the accretion of interstellar dust grains or synthesized *in situ*. Simulated hydrothermal processing in the presence of serpentinite appears to have a significant negative impact on the abundances of the amino acids serine and alanine relative to samples containing water alone. In contrast, the presence of pulverized Allende meteorite has a positive impact on the serine abundance relative to samples containing water alone, and a neutral-to-mildly positive impact on the abundances of all other amino acids detected in our experiments. These results also suggest that amino acid abundances may vary based on localized mineral inclusions.

Acknowledgments

Thank you to Scott A. Sandford for insightful discussions. Special thanks to Stephen Brown and Eugene Gerashchenko for the maintenance and operation of the Van de Graaff accelerator in the Radiation Effects Facility at GSFC.

Author Disclosure Statement

No competing financial interests exist.

Funding Information

This work was supported by the Emerging Worlds program, award number 19-EW19_2-0021, and NASA's Planetary Science Division Internal Scientist Funding Program through the Fundamental Laboratory Research (FLaRe) Work Package at NASA Goddard Space Flight Center. H.L.M., K.K.F., P.D.T., F.T.F., C.A.K., and M.T.T. were funded through the Center for Research and Exploration in Space Science and Technology II (CRESST II) cooperative agreement under award number 80GSFC21M0002.

Supplementary Material

Supplementary Figure S1
Supplementary Figure S2
Supplementary Figure S3
Supplementary Table S1

References

Aponte JC, Abreu NM, Glavin DP, et al. Distribution of aliphatic amines in CO, CV and CK carbonaceous chondrites and relation to mineralogy and processing history. *Meteorit Planet Sci* 2017a;52(12):2632–2646; doi: 10.1111/maps.12959

Aponte JC, Elsila JE, Glavin DP, et al. Pathways to meteoritic glycine and methylamine. *ACS Earth Space Chem* 2017b; 1(1):3–13; doi: 10.1021/acsearthspacechem.6b00014

Behr PR, Tribbett PD, Robinson TD, *et al*. Compaction of Porous H_2O Ice via Energetic Electrons. *ApJ* 2020;900(2): 147; doi: 10.3847/1538-4357/abad3f

Bernstein MP, Dworkin JP, Sandford SA, et al. Racemic amino acids from the ultraviolet photolysis of interstellar ice analogues. *Nature* 2002;416(6879):401–403; doi: 10.1038/416401a

Bernstein MP, Sandford SA, Allamandola LJ, et al. Organic compounds produced by photolysis of realistic interstellar and cometary ice analogs containing methanol. *ApJ* 1995; 454:327; doi: 10.1086/176485

Blitz L, Shu FH. The origin and lifetime of giant molecular cloud complexes. *ApJ* 1980;238:148; doi: 10.1086/157968

Briggs R, Ertem G, Ferris JP, et al. Comet halley as an aggregate of interstellar dust and further evidence for the photochemical formation of organics in the interstellar medium. *Orig Life Evol Biosph* 1992;22(5):287–307; doi: 10.1007/BF01810858

Brunauer S, Emmett PH, Teller E. Adsorption of gases in multimolecular layers. *J Am Chem Soc* 1938;60(2):309–319; doi: 10.1021/ja01269a023

Burton AS, Stern JC, Elsila JE, et al. Understanding prebiotic chemistry through the analysis of extraterrestrial amino acids and nucleobases in meteorites. *Chem Soc Rev* 2012;41(16): 5459–5472; doi: 10.1039/c2cs35109a

Chang S, Bunch TE. Clays and organic matter in meteorites. In (Cairns-Smith A. G and Hartman H. Cambridge.eds.) Clay Minerals and the Origin of Life: Cambridge University Press: Cambridge, UK, 1986, pp. 116–129.

Cobb AK, Pudritz RE. Nature's starships. I. Observed abundances and relative frequencies of amino acids in meteorites. *ApJ* 2014;783(2):140; doi: 10.1088/0004-637X/783/2/140

Cottin H, Szopa C, Moore MH. Production of hexamethylenetetramine in photolyzed and irradiated interstellar cometary ice analogs. *ApJ* 2001;561(1):L139–L142; doi: 10.1086/324575

de Marcellus P, Meinert C, Nuevo M, et al. Non-racemic amino acid production by ultraviolet irradiation of achiral interstellar ice analogs with circularly polarized light. *ApJ* 2011;727(2):L27; doi: 10.1088/2041-8205/727/2/L27

Elmasry W, Kebukawa Y, Kobayashi K. Synthesis of organic matter in aqueous environments simulating small bodies in the solar system and the effects of minerals on amino acid formation. *Life (Basel)* 2021;11(1):32; doi: 10.3390/life11010032

Elsila JE, Aponte JC, Blackmond DG, et al. Meteoritic amino acids: Diversity in compositions reflects parent body histories. *ACS Cent Sci* 2016;2(6):370–379; doi: 10.1021/acscentsci.6b00074

Gerakines PA, Moore MH, Hudson RL. Ultraviolet photolysis and proton irradiation of astrophysical ice analogs containing hydrogen cyanide. *Icarus* 2004;170(1):202–213; doi: 10.1016/j.icarus.2004.02.005

Glavin DP, Alexander C, Aponté JC, et al. Chapter 3 – The origin and evolution of organic matter in carbonaceous chondrites and links to their parent bodies. Primie Meteor Astero 2018;205–271; doi; 10.1016/B978-0-12-813325-5.00003-3

Glavin DP, Callahan MP, Dworkin JP, et al. The effects of parent body processes on amino acids in carbonaceous chondrites. Meteoritics and Planetary Science 2011;45:1948–1972; doi: 10.1111/j.1945-5100.2010.01132.x

Glavin DP, McLain HL, Dworkin JP, et al. Abundant extraterrestrial amino acids in the primitive CM carbonaceous chondrite Asuka 12236. Meteoritics & Planetary Science 2020;55(9):1979–2006; doi: 10.1111/maps.13560

Hagen W, Allamandola LJ, Greenberg JM, et al. Interstellar molecule formation in grain mantles: The laboratory analog experiments, results and implications. *Astrophys Space Sci* 1979;65(1):215–240.

Hänchen M, Prigiobbe V, Storti G, et al. Dissolution kinetics of fosteritic olivine at 90–150°C including effects of the presence of CO_2. *Geochimica et Cosmochimica Acta* 2006;70(17):4403–4416; doi: 10.1016/j.gca.2006.06.1560

Herbst E, van Dishoeck EF. Complex organic interstellar molecules. *Annu Rev Astron Astrophys* 2009;47(1):427–480; doi: 10.1146/annurev-astro-082708-101654

Hudson RL, Moore MH, Dworkin JP, et al. Amino acids from ion-irradiated nitrile containing ices. *Astrobiology* 2008;8(4):771–779; doi: 10.1089/ast.2007.0131

Hudson RL, Lewis AS, Moore MH, et al. (2009) "Enigmatic Isovaline: Investigating the Stability, Racemization, and Formation of a Non-Biological Meteoritic Amino Acid." Astronomical Society of the Pacific Bioastronomy 2007: Molecules, Microbes, and Extraterrestrial Life. Astronomical Society of the Pacific, p. 157.

Hulett HR. Formaldehyde and ammonia as precursors to prebiotic amino acids. *Science* 1971;174(4013):1038–1039.

Kasamatsu T, Kaneko T, Saito T, et al. Formation of organic compounds in simulated interstellar media with high energy particles. *Bull Chem Soc Jpn* 1997;70(5):1021–1026; doi: 10.1246/bcsj.70.1021

Kebukawa Y, Chan QH, Tachibana S, et al. One-pot synthesis of amino acid precursors with insoluble organic matter in planetesimals with aqueous activity. *Science Advances* 2017;3(3):e1602093–e1602548; doi: 10.1126/sciadv.1602093

Kleber M, Bourg IC, Coward EK, et al. Dynamic interactions at the mineral–organic matter interface. *Nat Rev Earth Environ* 2021;2(6):402–421; doi: 10.1038/s43017-021-00162-y

Li Z, Cheng H, Fu Y, et al. Dissolution property of serpentine surface and the effect on particle–particle interaction behavior in solution. *Minerals* 2023;13(6):799; doi: 10.3390/min1306079

Materese CK, Gerakines PA, Hudson RL. Laboratory studies of astronomical ices: Reaction chemistry and spectroscopy. *Acc Chem Res* 2021;54(2):280–290; doi: 10.1021/acs.accounts.0c00637

Materese CK, Nuevo M, Sandford SA, et al. The production and potential detection of hexamethylenetetramine-methanol in space. *Astrobiology* 2020;20(5):601–616; doi: 10.1089/ast.2019.2147

Moore MH, Hudson RL, Gerakines PA. Mid- and far-infrared spectroscopic studies of the influence of temperature, ultraviolet photolysis and ion irradiation on cosmic-type ices. *Spectrochim Acta A Mol Biomol Spectrosc* 2001;57(4):843–858; doi: 10.1016/S1386-1425(00)00448-0

Muñoz Caro GM, Meierhenrich UJ, Schutte WA, et al. Amino acids from ultraviolet irradiation of interstellar ice analogues. *Nature* 2002;416(6879):403–406.

Muñoz Caro GM, Schutte WA. UV-photoprocessing of interstellar ice analogs: New infrared spectroscopic results. *A&A* 2003;412(1):121–132; doi: 10.1051/0004-6361:20031408

Nuevo M, Auger G, Blanot D, et al. A detailed study of the amino acids produced from the vacuum UV irradiation of interstellar ice analogs. *Orig Life Evol Biosph* 2008;38(1):37–56.

Nuevo M, Chen Y-J, Yih T-S, et al. Amino acids formed from the UV/EUV irradiation of inorganic ices of astrophysical interest. *Adv Space Res* 2007;40(11):1628–1633; doi: 10.1016/j.asr.2007.04.056

Oba Y, Takano Y, Naraoka H, et al. Deuterium fractionation upon the formation of hexamethylenetetramines through photochemical reactions of interstellar ice analogs containing deuterated methanol isotopologues. *ApJ* 2017;849(2):122.

Öberg KI. Photochemistry and Astrochemistry: Photochemical pathways to interstellar complex organic molecules. *Chem Rev* 2016;116(17):9631–9663.

Pavlov AA, McLain HL, Glavin DP, et al. Rapid radiolytic degradation of amino acids in the martian shallow subsurface: Implications for the search for extinct life. *Astrobiology* 2022;22(9):1099–1115.

Qasim D, McLain HL, Aponte JC, et al. Meteorite parent body aqueous alteration simulations of interstellar residue analogs. *ACS Earth Space Chem* 2023;7(1):156–167.

Shock EL, Schulte MD. Amino-acid synthesis in carbonaceous meteorites by aqueous alteration of polycyclic aromatic hydrocarbons. *Nature* 1990;343(6260):728–731.

Sing KSW. Adsorption methods for the characterization of porous materials. *Advances in Colloid and Interface Science* 1998;76–77:3–11.

Takano Y, Takahashi J, Kaneko T, et al. Asymmetric synthesis of amino acid precursors in interstellar complex organics by circularly polarized light. *Earth Planet Sci Lett* 2007;254(1–2): 106–114.

Vinogradoff V, Bernard S, Le Guillou C, et al. Evolution of interstellar organic compounds under asteroidal hydrothermal conditions. *Icarus* 2018;305:358–370.

Vinogradoff V, Le Guillou C, Bernard S, et al. Influence of phyllosilicates on the hydrothermal alteration of organic matter in asteroids: Experimental perspectives. *Geochim Cosmochim Acta* 2020a;269:150–166.

Vinogradoff V, Remusat L, McLain HL, et al. Impact of phyllosilicates on amino acid formation under asteroidal conditions. *ACS Earth Space Chem* 2020b;4(8):1398–1407.

Wogelius RA, Walther JV. Olivine dissolution at 25°C: Effects of pH, CO_2, and organic acids. *Geochimica et Cosmochimica Acta* 1991;55(4):943–954.

Address correspondence to:
Christopher K. Materese
Solar System Exploration Division
NASA Goddard Space Flight Center
8800 Greenbelt Rd
Greenbelt
MD 20771-0003
USA

E-mail: Christopher.K.Materese@nasa.gov

Submitted July 17, 2024
Accepted November 1, 2024
Associate Editor: Sherry L. Cady

Abbreviations Used

ABA = aminobutyric acid
AIB = aminoisobutyric acid
BET = Brunauer–Emmett–Teller
HMT = hexamethylenetetramine
HPLC = high-performance liquid chromatography
MRM = multiple reaction monitoring
UHPLC = Ultra High Precision Liquid Chromatography